AER 1513 State Estimation Project: Attitude Determination for Small Satellites

Cody Santing - 1000600174, Xiaozheng Xu - 1001160548

University of Toronto Institute for Aerospace Studies

I. INTRODUCTION

The attitude of a satellite can be considered its orientation in 3D space. Attitude control is essential for space missions for a few reasons. One is for targeting, specifically in the case where an instrument needs to observe an area of interest. For example, the UTIAS Space Flight Laboratory (SFL) has developed the GHGSAT-D satellite, which is used to monitor green house gas emitters on Earth [5]. It is imperative GHGSAT-D point to the correct target and accurately otherwise no meaningful data can be collected. It is also important that a satellite be in an attitude such that sufficient data transfer rates to listening ground stations can be achieved. Antennas are not perfectly omnidirectional, so it is necessary to point the antenna in such a way that a higher data rate can be achieved. There are multiple approaches to rotating the spacecraft into the desired attitude, however the focus of this paper is determining the current attitude using on-board sensor data. A number of sensors will be modeled and the Extended Kalman Filter (EKF) approach utilizing quaternions will be shown. Results of the EKF on simulation and actual on-board data will be shown and a batch estimation method will be applied to simulation results for comparison. Additionally, different attitude sensor interactions will be shown.

A. EXISTING LITERATURE

The extended Kalman filter is used in the attitude determination of small satellites using the available sensors on board. While star trackers are the most accurate attitude sensor, attitude estimation has been done using a combination of a magnetometer and sun sensors [4] and even using only magnetometers [3].

This project implements the EKF with body rates from an inertial measurement unit (IMU), magnetometer, and star tracker.

II. MOTION MODEL

The state vector is represented as a quaternion, q_k. The motion model of the spacecraft is found in Equation 1. T is the time interval between measurements and w_k is the angular speed in the inertial frame.

$$q_k = q_{k-1} + \frac{T}{2} q_{k-1} \circ \begin{bmatrix} 0 \\ w_k \end{bmatrix} \tag{1}$$

Note, that the derivative of a quaternion is found in Equation 2, thus the motion model is taking the current state and simply updating based on the current angular motion.

$$\frac{1}{2} q_{k-1} \circ \begin{bmatrix} 0 \\ w_k \end{bmatrix} \tag{2}$$

The $\circ$ operator is a quaternion multiplication, defined as:

$$q \circ p = \begin{bmatrix} q_0 & -q_1 & -q_2 & -q_3 \\ q_1 & q_0 & -q_3 & q_2 \\ q_2 & q_3 & q_0 & -q_1 \\ q_3 & -q_2 & q_1 & q_0 \end{bmatrix} \begin{bmatrix} p_0 \\ p_1 \\ p_2 \\ p_3 \end{bmatrix} \tag{3}$$

The operation represents compounding the two rotations represented by the quaternions. The result is another quaternion of that compound.

III. SENSOR MODELS

There are a variety of sensors used for assisting in estimating spacecraft attitude, This paper will focus on a few of them, namely the star tracker, sun sensor, magnetometer, and IMU. A star tracker takes images of the sky and compares the relative position of the observed stars to an on-board data base in order to match similar patterns. The most accurate sensor is the star tracker which directly returns a quaternion already in the star tracker frame. Thus, the measurement model for a star tracker is simply:

$$q_s = q_b \circ q_{sb} \tag{4}$$

where q_{sb} is the rotation from the spacecraft body frame to the star tracker frame.

The magnetometer measures the magnetic field vector and strength in the spacecraft body frame, B_b. The magnetic field vector in the inertial frame, B_i, can be predicted given the spacecraft's location above Earth using a universal model magnetic field, such as the International Geomagnetic Reference Field (IGRF). C_{bi} acts as the rotation matrix from the inertial frame to the body frame:

$$B_b = C_{bi} B_i \tag{5}$$

There are typically sun sensors on all faces. They detect the general direction of the sun relative to the spacecraft. Thus, for a simple cubic model of a spacecraft, there is 6 sun sensors. S_i is the inertial sun vector at the current time. C_{si} is the rotation matrix from the inertial frame to the body frame:

$$S_b = C_{si} S_i \tag{6}$$

IV. SIMULATION DATA

To easily test sensor models and state estimation techniques, it is useful to first run on simulation data rather than directly on a spacecraft. AGI's Systems Tool Kit (STK) was used to simulate a spacecraft in Low-Earth Orbit. Simulations were run for a three month period with data collected at one second intervals. The spacecraft's attitude quaternions for each time step were

generated, which acts as the state vector and ground truth. A Nadir-pointing attitude was set as the desired attitude throughout the duration of the simulation. Additionally, the angular velocity in a vector form as well as the Earth's magnetic field parameters at the current position were generated.

To avoid a computationally costly simulation, sensors were not modeled in the simulations. Rather, zero-mean Gaussian noise was added to the ground truth at each time step. The result acts as the sensor readings.

V. ATTITUDE DATA FROM SPACECRAFT

In order to test and verify the approach, on-orbit data of an SFL spacecraft is used. The data used includes the state vector, which was estimate using an on-board Extended Kalman Filter (EKF), star tracker measurements, estimated body rates, the magnetic field in the inertial frame, B_i, the magnetic field in the spacecraft body frame, B_b, and sun sensor measurements. The state vector acts as a ground truth in the absence of an actual ground truth.

VI. EXTENDED KALMAN FILTER

The EKF was implemented with the state as the quaternion that represents the rotation of the spacecraft with respect to the inertial frame.

$$x_k = \begin{bmatrix} q_0 \\ q_1 \\ q_2 \\ q_3 \end{bmatrix} \tag{7}$$

A. NOISE VALUES

The process noise from the IMU is:

$$\begin{aligned} \mathbf{Q} &= \begin{bmatrix} w1_{var} & 0 & 0 \\ 0 & w2_{var} & 0 \\ 0 & 0 & w3_{var} \end{bmatrix} \\ &= \begin{bmatrix} 0.0005(rad/s)^2 & 0 & 0 \\ 0 & 0.0005(rad/s)^2 & 0 \\ 0 & 0 & 0.0005(rad/s)^2 \end{bmatrix} \end{aligned} \tag{8}$$

The measurement noise for the magnetometer is:

$$\mathbf{R}_{mag} = \begin{bmatrix} mag_{var} & 0 & 0 \\ 0 & mag_{var} & 0 \\ 0 & 0 & mag_{var} \end{bmatrix} = \begin{bmatrix} 0.03 & 0 & 0 \\ 0 & 0.03 & 0 \\ 0 & 0 & 0.03 \end{bmatrix} \tag{9}$$

The measurement noise for the star tracker is:

$$\begin{aligned} \mathbf{R}_{qs} &= \begin{bmatrix} qs_{var} & 0 & 0 & 0 \\ 0 & qs_{var} & 0 & 0 \\ 0 & 0 & qs_{var} & 0 \\ 0 & 0 & 0 & qs_{var} \end{bmatrix} \\ &= \begin{bmatrix} 2e-5 & 0 & 0 & 0 \\ 0 & 2e-5 & 0 & 0 \\ 0 & 0 & 2e-5 & 0 \\ 0 & 0 & 0 & 2e-5 \end{bmatrix} \end{aligned} \tag{10}$$

The total noise matrix for the measurements

$$\mathbf{R} = diag([\mathbf{R}_{mag}; \mathbf{R}_{qs}]) \tag{11}$$

If the star tracker is unavailable at any given time stamp due to the orientation of the spacecraft, $\mathbf{R}$ will only consist of $\mathbf{R}_{mag}$.

B. JACOBIANS

For the motion model,

$$\begin{aligned} \check{\mathbf{x}_k} &= f(\hat{\mathbf{x}}_{k-1}, \mathbf{w}_k, 0) \\ &= \hat{\mathbf{x}}_{k-1} + \frac{T}{2}\hat{\mathbf{x}}_{k-1} \circ [0; \mathbf{w}_k] = \begin{bmatrix} \check{q0}_k \\ \check{q1}_k \\ \check{q2}_k \\ \check{q3}_k \end{bmatrix} \end{aligned} \tag{12}$$

The Jacabian of f,

$$\mathbf{F}_k = \frac{T}{2}\begin{bmatrix} \frac{2}{T} & -w1 & -w2 & -w3 \\ w1 & \frac{2}{T} & w3 & -w2 \\ w2 & -w3 & \frac{2}{T} & w1 \\ w3 & w2 & -w1 & \frac{2}{T} \end{bmatrix} \tag{13}$$

The Jacobian of the noise

$$\mathbf{W}_k = \frac{T}{2}\begin{bmatrix} -q1 & -q2 & -q3 \\ q0 & -q3 & q2 \\ q3 & q0 & -q1 \\ -q2 & q1 & q0 \end{bmatrix} \tag{14}$$

The Jacobian G_k is the combination of the Jacobian for the measurement model of the magnetometer and the star tracker. The Jacobian for the measurement noise N_k is just the identity matrix.

C. EXTENDED KALMAN FILTER EQUATIONS

The equations for the EKF are as follows:
Predictor step:

$$\begin{aligned} \check{\mathbf{P}}_k &= \mathbf{F}_{k-1}\hat{\mathbf{P}}_{k-1}\mathbf{F}_{k-1}^T + \mathbf{W}_k\mathbf{Q}_k\mathbf{W}_k^T \\ \check{\mathbf{x}_k} &= f(\hat{\mathbf{x}}_{k-1}, \mathbf{v}_k, 0) \end{aligned} \tag{15}$$

Kalman Gain:

$$\begin{aligned} \mathbf{K}_k &= \check{\mathbf{P}}_k\mathbf{G}_k^T(\mathbf{G}_k\check{\mathbf{P}}_k\mathbf{G}_k^T + \mathbf{N}_k\mathbf{R}_k\mathbf{N}_k^T)^{-1} \\ \hat{\mathbf{P}}_k &= (\mathbf{I} - \mathbf{K}_k\mathbf{G}_k)\check{\mathbf{P}}_k \end{aligned} \tag{16}$$

Corrector step:

$$\hat{\mathbf{x}}_k = \check{\mathbf{x}}_k + \mathbf{K}_k(\mathbf{y}_k - g(\check{\mathbf{x}}_k, 0)) \tag{17}$$

To accommodate multiple measurements, $\mathbf{y}_p$ is extended to be

$$\mathbf{y}_p = g(\hat{\mathbf{x}}_k, 0) = \begin{bmatrix} \check{B}_{1,k} \\ \check{B}_{2,k} \\ \check{B}_{3,k} \\ \check{qs}_{0,k} \\ ... \\ \check{qs}_{3,k} \end{bmatrix} \tag{18}$$

At the end of each step, the quaternion state x_k is normalized so it can remain a unit quaternion. This is done by dividing x_k by its magnitude.

D. MATLAB RESULTS ON SIMULATED DATA

The EKF was run on the simulated data with varying combinations of sensors. First, the IMU and magnetometer. The results and angle error are found below:

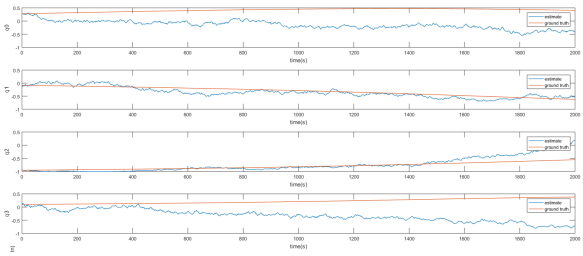

Fig. 1: Resulting estimates of quaternions using body rates and magnetometer in simulation

It can be seen that there is a growing inaccuracy across multiple quaternions. The overall angle result reflects this:

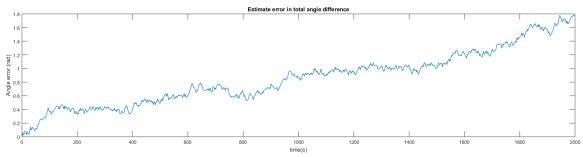

Fig. 2: Angle error using body rates and magnetometer

The magnetometer is unable to correct the growing error of the IMU. Next, the star tracker and body rates were used as inputs to the EKF:

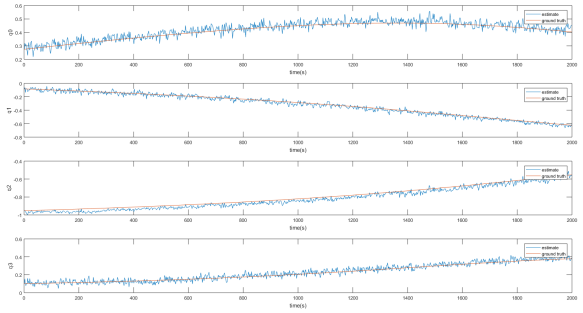

Fig. 3: Resulting estimates of quaternions using body rates and star tracker in simulation

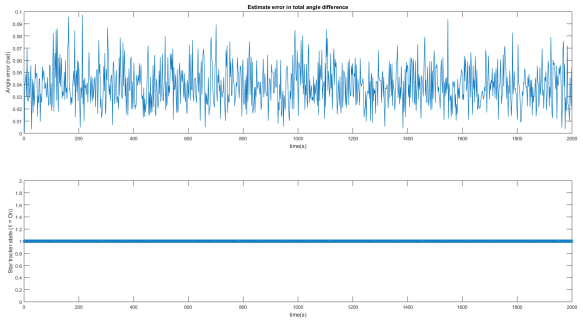

Fig. 4: Angle error using body rates and star tracker

As seen in Figure 4, the angle error is very low and is not growing over time. The star tracker successfully contains the error and simulations confirm the high accuracy of the star tracker.

Combining the IMU, star tracker and magnetometer give interesting results. The star tracker is not consistently used. This allows observation of the star tracker's correction to the estimate.

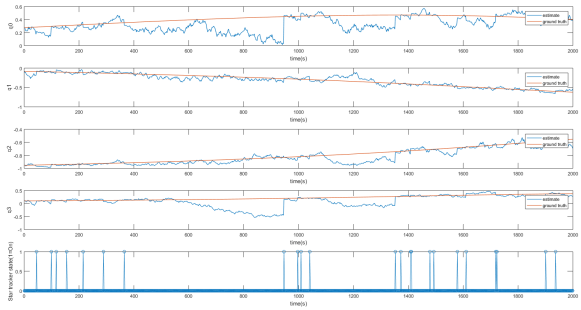

Fig. 5: Resulting estimates of quaternions using body rates, star tracker and magnetometer in simulation

Using only the magnetometer and IMU, the error is quick to grow. There are drastic corrections taking place when the star tracker is in use due to it's high accuracy:

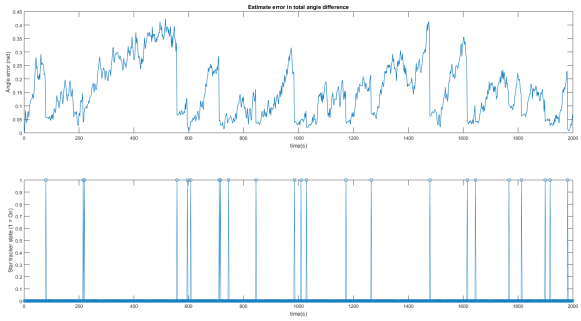

Fig. 6: Angle error using body rates, star tracker and magnetometer

E. MATLAB RESULTS ON SPACECRAFT DATA

Simulations are useful for inital verification, however it is more beneficial to run estimates using actual on-board data for comparison and to give an idea of true accuracy.

As a way to verify sensors are being modeled correctly, a simple estimation relying on dead reckoning using only the angular body rates from the state vector was run, producing the results below:

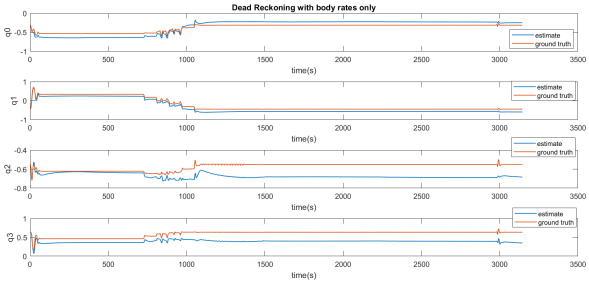

Fig. 7: Resulting estimates of quaternions using only body rates

Note that in this scenario, the spacecraft is rotating from one attitude to another between the 600 and 1200 second marks. The minimum angle error between the dead reckoning and state vector ground truth is found by converting the state quaternions into a rotation vector. The results for the same scenario are found below:

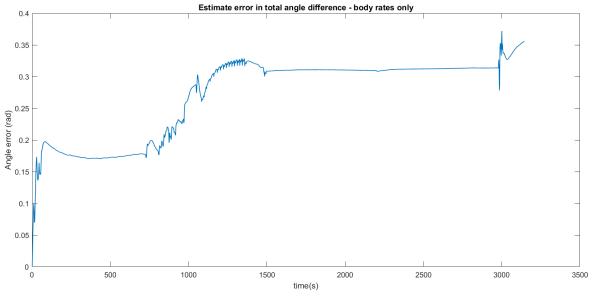

Fig. 8: Angle error using only body rates

When adding in the magnetometer measurements, the effects in Figures 9 and 10 are produced. The accuracy is maintained, even during the maneuver between the 600 and 1200 second marks. However, as time goes on, the angle error continues to grow, despite the magnetometer's attempts to correct.

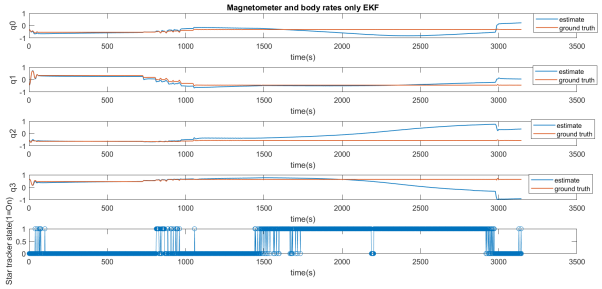

Fig. 9: Resulting estimates of quaternions using body rates and magnetometer

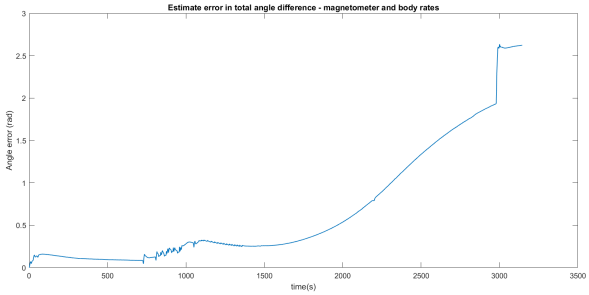

Fig. 10: Angle error using only body rates and magnetometer

Using the star tracker only when it's available, specifically where the star tracker is pointed away from Earth, the drifting error from the body rates is corrected, as seen below:

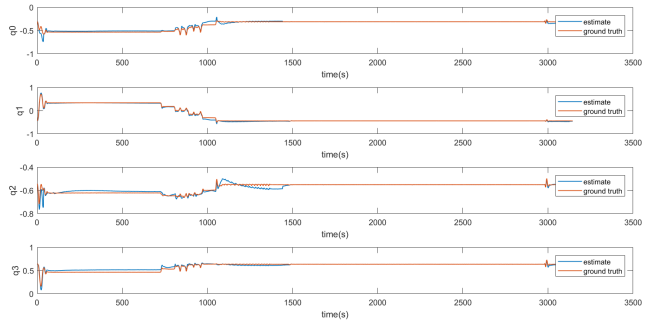

Fig. 11: Star tracker and body rates results

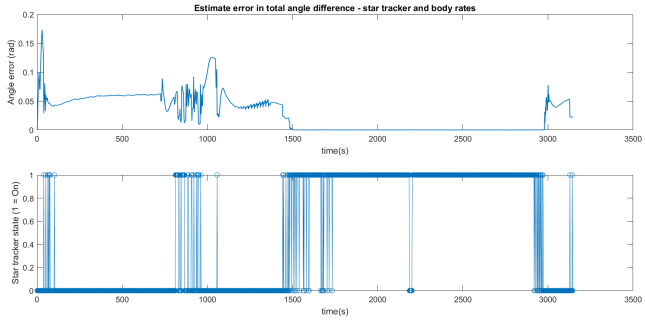

Fig. 12: Star tracker and body rates angle error

As mentioned earlier, the star tracker is quite accurate such that when it is on, the error is very close to zero, with only some deviation during the maneuver.

When both the star tracker and magnetometer is used, the results are:

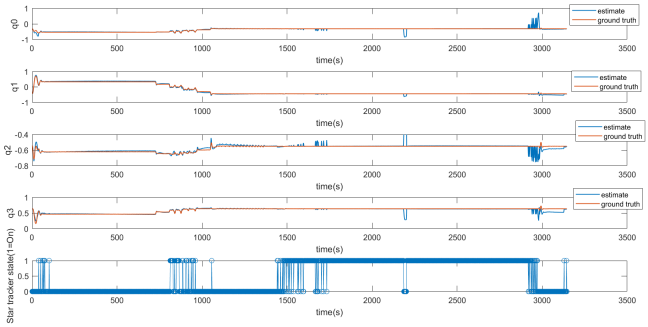

Fig. 13: Magnetometer, Star tracker and body rates EKF results with noise variance of 0.03

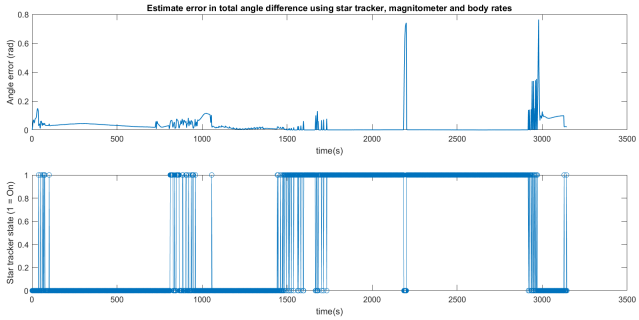

Fig. 14: Magnetometer, Star tracker and body rates EKF angle error with noise variance of 0.03

The oscillation in the angle error when the star tracker switches between on and off is caused by the magnetometer having a larger measurement error than the star tracker. However, since the body rates are more accurate than the magnetometer, it should be possible to reduce the EKF error by favoring the body rates measurement more in the absence of star tracker data. When the noise variance for the magnetometer is changed to 3 instead of 0.03, the error becomes smaller as shown in the figure below

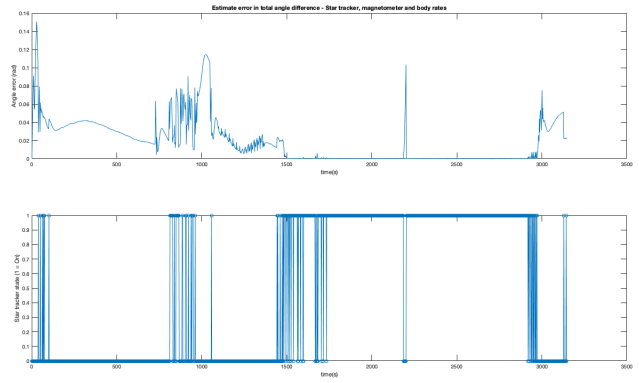

Fig. 15: Magnetometer, Star tracker and body rates EKF angle error with noise variance of 3

Generally, the EKF results using actual data match the results of the simulation. As there was a maneuver performed during the secnario, further information is gained of the EKF behavior.

VII. BATCH METHOD

For comparison and to see the effectiveness of the EKF method relative to another method, a Batch estimation approach is used. This utilizes all data of a given set to calculate the state at any given time step. For this reason, the Batch method is not suitable for on-board state estimation as the required computing power is too large for conventional spacecraft.

A. SIMULATION RESULTS

The Batch method was used on the simulation data and is thus compared to the EKF simulation results. First, estimation using the magnetometer and IMU were completed:

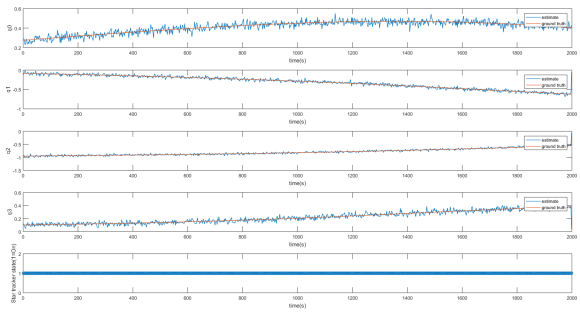

Fig. 16: Resulting batch estimates of quaternions using body rates and star sensor

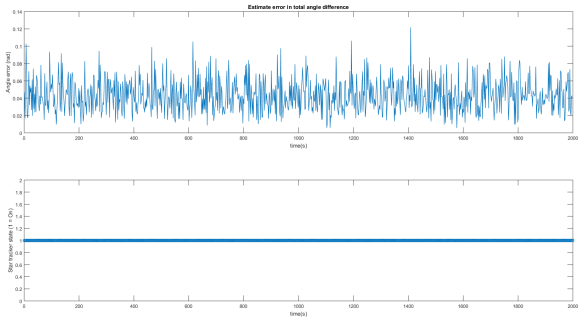

Fig. 17: Batch angle error using only body rates and star sensor

Similar to the EKF method, the batch estimate consisting of a star sensor and the IMU to get body rates is quite accurate. The angle error is within 0.13 radians throughout the simulation time.

Due to the high computational load, a Batch estimation is more suited for a ground station where computing power is effectively limitless. On-board state estimation is better suited for the EKF.

VIII. CONCLUSION

It has been shown how a variety of sensors, specifically an IMU, magnetometer and star tracker, can be used to estimate the

attitude of a small satellite. Simulations were run to first verify the approach followed by analysis using on-board satellite data from an operational mission. The analysis of on-board data confirmed the simulation results. Additionally, different sensor combinations and interactions were shown. Results reflect the high accuracy of star trackers. A comparison between the Extended Kalman Filter and Batch state estimation approaches was made. Future avenues of research can include adding sun sensors to experiments and simulations. More Batch estimate experiments would be beneficial to compare different sensor interactions across the methods. Also, due to the similarly high Batch accuracy, it could be beneficial to develop an approach that uses the EKF on-board with periodic correction or confirmation from a Batch estimate made using telemetry data collected over a longer period of time at a ground station.

REFERENCES

[1] Michael Strohmeier: Quaternion based Extended Kalman Filter https://wuecampus2.uni-wuerzburg.de/moodle/pluginfile.php/1109745/mod_resource/content/1/QEKF_Floatsat_WS16.pdf.

[2] Kevin P. Corbley: Attitude Control Technologies for Smaller Satellites Enable Complex Applications in Earth Observation, Space Astronomy and Science Research http://eijournal.com/print/articles/attitude-control-technologies-for-smaller-satellites-enable-complex-applications-in-earth-observation-space-astronomy-and-science-research.

[3] Jason D. Searcy. *Magnetometer-only attitude determination with application to the M-SAT mission*. 2011. http://scholarsmine.mst.edu/masters_theses/6892/

[4] Todd E. Humphreys. *Attitude Determination for Small Satellites Using Magnetometer and Solar Panel Data*

[5] Microsatellites: GHGSat-D (Claire) https://www.utias-sfl.net/?page$_id = 1254$